J Solid State Electrochem (2010) 14:2267–2274
DOI 10.1007/s10008-010-1067-z

ORIGINAL PAPER

PMo_{12}-functionalized Graphene nanosheet-supported PtRu nanocatalysts for methanol electro-oxidation

Haiyong Li · Xiaohua Zhang · Haili Pang · Changting Huang · Jinhua Chen

Received: 17 December 2009 / Revised: 16 March 2010 / Accepted: 30 March 2010 / Published online: 20 April 2010

Abstract Graphene nanosheets, synthesized by a modified Hummers method, have been functionalized by PMo_{12}, and used as the supports of the PtRu nanoparticles. The electrocatalytic properties of the resultant nanocatalysts (PtRu/PMo_{12}-Graphene) for methanol electro-oxidation have been evaluated by cyclic voltammetry and chronoamperometry. The micrograph and the elemental composition have also been investigated by transmission electron microscopy and energy dispersive X-ray spectroscopy. The results suggest that the addition of PMo_{12} benefits the high dispersion of graphene nanosheets in the water and the uniform dispersion of the PtRu nanoparticles on the graphene nanosheets, and the PtRu/PMo_{12}-Graphene catalysts have higher electrocatalytic activity and better electrochemical stability for methanol oxidation compared to the PtRu/Graphene catalysts.

Keywords Graphene nanosheet · PMo_{12} · Methanol electro-oxidation · Electrocatalyst

Introduction

Direct methanol fuel cells (DMFCs), as promising power sources for portable electrical devices, have attracted more and more attention in the past decades due to their high energy-conversion efficiency, low operating temperature, as well as the simple handling and processing of fuel [1]. However, compared with hydrogen-fed fuel cells, one of the main challenges, which DMFCs have to face, is the slow anode dynamics and the poisoning tendency of the anodic catalysts by some adsorbed intermediates during the processes of methanol oxidation, such as CO_{ads}. Consequently, enormous efforts have been devoted towards the improvement of the activity and endurance of the anodic electrocatalysts [2]. For this purpose, lots of catalysts including Pt, Pt-based alloys, and oxides have been proposed for the oxidation of methanol. Among them, bimetallic PtRu catalyst is considered to be the most promising anodic catalyst for DMFCs [3]. In addition, supporting materials, which have a large effect on the particle size and distribution of the supported nanocatalysts, have also been proven to be essential to the electrocatalysts to achieve high catalytic activity for methanol electro-oxidation [4]. It is well known that various carbon materials, such as Vulcan XC-72R carbon black [5], carbon nanotubes (CNTs) [6, 7], graphitic carbon nanofibers (GNFs) [8, 9], carbon nanohorns [10], carbon nanoporous arrays [11, 12], carbon microbeads [13], and mesoporous carbons [14] have been used as the catalyst supports in DMFCs.

Recently, graphene, a single-atom-thick sheet of hexagonally arrayed sp^2-bonded carbon atoms, has been characterized as "the thinnest material in our universe" [15] and received tremendous attention in fuel cell application due to the particular electronic conductivity and extremely high specific surface area (theoretical specific surface area of 2,630 m^2/g) [16]. Unfortunately, it is so difficult to obtain a truly single sheet of graphene in practice that researchers have focused their efforts on several or even tens of graphene nanosheets. Many papers have reported that graphene nanosheet-supported Pt or Pt–Ru nanoparticles displayed excellent electrocatalytic activity for methanol

H. Li · X. Zhang (✉) · H. Pang · C. Huang · J. Chen (✉)
State Key Laboratory of Chemo/Biosensing and Chemometrics,
College of Chemistry and Chemical Engineering,
Hunan University,
Changsha 410082, People's Republic of China
e-mail: guoxin512@tom.com
e-mail: chenjinhua@hnu.cn

oxidation [17]. Wang et al. prepared graphene–metal particle nanocomposites in a water–ethylene glycol system using graphene oxide as the precursor and metal nanoparticles (Au, Pt, and Pd) as building blocks and investigated the potential application of graphene–Pt composites in direct methanol fuel cells [18]. Li et al. prepared Pt/graphene nanocomposites via reduction of graphite oxide and H_2PtCl_6 in one pot, and good catalytic performance of the composites toward methanol oxidation was observed [19]. Yoo et al. demonstrated that graphene nanosheet (GNS), synthesized through chemical reduction of exfoliated graphite oxide, gives rise to an extraordinary modification to the properties of Pt cluster electrocatalysts supported on it, and the Pt/GNS electrocatalyst exhibits an unusually high activity for methanol oxidation reaction compared to Pt/carbon black catalyst [20]. These imply that graphene nanosheets should be favorable candidates for the catalyst supports in methanol oxidation [21].

Up to date, graphene nanosheets have been produced either by mechanical exfoliation via repeated peeling of highly ordered pyrolytic graphite (HOPG) or by chemical oxidation of graphite [22–26]. As recently demonstrated, considering the facile solution processing, graphene nanosheets have been usually prepared by chemical reduction of graphene oxide in solution [27, 28]. However, the electronic conductive graphene nanosheets, obtained through the chemical reduction of the non-electronic conductive graphene oxide, have few oxygen-containing groups and could not readily disperse in aqueous solution [29], which would be disadvantageous for the assembly and dispersion of Pt or PtRu nanoparticles. Besides, because of the Van der Waals interactions, the as-reduced graphene nanosheets tend to form irreversible agglomerates. In order to obtain water soluble or dispersible graphene as individual sheets, attaching some molecules or polymers onto the sheets is a usable approach to reduce the aggregation [30, 31].

Heteropolyacids (HPAs) are a subset of the polyoxometalates, which are very strong Bronsted acids with very high proton conduction, and also exhibit fast reversible multi-electron redox behavior under mild conditions [32]. Many encouraging studies provide evidence that HPAs, in combination with Pt or PtRu, could act as promoters in the methanol electro-oxidation process on a fuel cell anode [33, 34]. Keggin-type heteropolyanions of molybdenum ($H_3PMo_{12}O_{40}$, PMo_{12}), a typical HPAs, have been attractive in surface chemical modification of catalyst support because of their ability to form self-assembled monolayers on common solid electrode substrates, especially on various carbon-based material and metal surface with high immobilization strength [35–37]. PMo_{12} has been preferred as a soluble molecular species in catalysis and biomedicine. The self-assembling and negatively charged nature of PMo_{12} monolayer is desirable for use in carbon-based supports to improve the dispersion and stability of nanoparticles supported on such matrix. However, functionalization of graphene nanosheets through strong chemisorption using PMo_{12} has rarely been addressed in the literatures, although there are some publications in the field of carbon nanotubes [38].

In this paper, graphene nanosheets were successfully prepared through chemical reduction of graphite oxide following the procedure described in Ref. [39, 40] and functionalized by PMo_{12}. And then, the PMo_{12}-functionalized graphene nanosheets (PMo_{12}-Graphene) were used as new catalyst support for high dispersion of PtRu nanoparticles. The resulting PtRu catalysts (PtRu/PMo_{12}-Graphene) exhibit improved performance for methanol electro-oxidation.

Experimental section

Synthesis of PMo_{12}-functionalized Graphene nanosheets

Graphene nanosheets were prepared through chemical reduction of graphite oxide (GO), which was synthesized from graphite powder (SP-1 grade 325 mesh, Alfa Inc.) by a modified Hummers method [39]. In brief, the suspension of exfoliated GO in pure water was reduced with hydrazine hydrate at 100 °C with stirring for 24 h, followed by vacuum filtration and washed with doubly distilled water and methanol for several times. Then, 100 mg of graphene nanosheets and 100 mg of PMo_{12} were dispersed in 200 mL of doubly distilled water with ultrasonic treatment for 24 h. The suspension was then filtrated and washed with doubly distilled water for several times, and finally dried at 40 °C in vacuum. The obtained product was denoted as PMo_{12}-Graphene.

Preparation of PtRu/PMo_{12}-Graphene and PtRu/Graphene catalysts

Taking H_2PtCl_6 and $RuCl_3$ as the precursors, the PtRu/PMo_{12}-Graphene (20 wt.% PtRu on the PMo_{12}-Graphene, the atomic ratio of Pt to Ru was approximately 1:1) electrocatalysts were prepared by microwave (MAS-II) irradiation method in ethylene glycol (EG) solution. In a typical procedure, 25 mL of EG was loaded into a 50-mL round-bottom flask, and 20 mg of PMo_{12}-Graphene prepared above was then added. The mixture was ultrasonically treated for 1 h. Then 0.88 mL of 19.3 mM H_2PtCl_6 $6H_2O$, 0.44 mL of 38.3 mM $RuCl_3$, and a definite volume of KOH (0.4 M) were added. The suspension was vigorously stirred for another 1 h, and then irradiated in a

microwave oven (800 W) at 120 °C for 30 min. The resulting product was filtered and washed with doubly distilled water and acetone for several times in turn and finally dried at 40 °C in vacuum overnight. For comparison, the PtRu/Graphene electrocatalysts without PMo_{12} modification were prepared by the same process described above. The metal content of the PtRu/PMo_{12}-Graphene catalyst and the PtRu/Graphene catalyst, determined by inductively coupled plasma-atom emission spectroscopy (ICP-AES), is equal to about 18.59 wt.% (Pt:Ru=1:0.9) and 17.18 wt.% (Pt:Ru=1:0.75), respectively.

Catalyst characterization

Morphology and microstructure of the graphene nanosheets and the catalysts were characterized by scanning electron microscopy (SEM, JSM-6700F), transmission electron microscopy (TEM, JEM-3010), and X-ray diffraction (XRD, D/MAX-RA), respectively. Brunauer Emmett Teller Procedure (BET, ASAP 2020 M+C) was used for surface area analysis of the graphene nanosheets. Elemental composition of the PtRu/PMo_{12}-Graphene catalysts was investigated by energy dispersive X-ray spectroscopy (EDS, Vantage 4105, NORAN).

Electrochemical measurement

The electrochemical properties of the PtRu/PMo_{12}-Graphene and PtRu/Graphene catalysts were investigated in 0.5 M H_2SO_4+1.0 M CH_3OH or 0.5 M H_2SO_4 aqueous solutions by typical electrochemical methods at 25 °C, carried out on a CHI660A electrochemical working station (Chenhua Instrument Company of Shanghai, China). A conventional three-electrode cell was employed with platinum wire as the counter electrode and a saturated calomel electrode (SCE) as the reference electrode, respectively. The glassy carbon electrode (GC) loaded with a definite mass of catalyst with an exposure area of 0.196 cm^2 was used as the working electrode. For preparing the PtRu/PMo_{12}-Graphene/GC electrode, 2 mg of PtRu/PMo_{12}-Graphene was first ultrasonically treated for 30 min in 2 mL fresh doubly distilled water, then 30 μL of the solution prepared above was transferred onto the surface of the GC electrode by a micro-syringe. After dried in air, the working electrode was coated with 3 μL of 0.5 wt.% Nafion ethanol solution. The preparation of PtRu/Graphene/GC electrode has a similar procedure.

For CO-stripping voltammetry, pure CO was first bubbled into the electrolyte for CO adsorption onto the electrode surface for 20 min. Subsequently, a N_2 purge was applied to remove the CO dissolved in the electrolyte before the stripping peak was measured.

Results and discussion

Characterization of PMo_{12}-Graphene and PtRu/PMo_{12}-Graphene catalyst

The micrographs and structure information of graphene oxide and graphene nanosheets were investigated by SEM, TEM, and XRD, respectively, and the corresponding results are show in Fig. 1. Figure 1a exhibits the SEM image of the graphene oxide sheets, some wrinkles can be obviously observed. That is because graphite oxide sheets tend to congregate together to form multilayer agglomerates [41]. From Fig. 1b and c (SEM and TEM images of the graphene nanosheets, respectively), the individual graphene nanosheets extending from the outer surface can be observed with more wrinkles on the graphene nanosheets, which may be important for preventing aggregation of graphene and maintaining high surface area [42]. The surface area of the graphene measured by the N_2 absorption Brunauer–Emmett–Teller (BET) method is about 450 m^2/g, much larger than that of carbon black XC-72 (180 m^2/g). This might have contributed to graphene nanosheets as promising catalyst support for fuel cell. To further characterize graphene oxide and graphene nanosheets, XRD was carried out and the corresponding results are presented in Fig. 1d. In Fig. 1d, the graphite (002) diffraction peak at around 25.2° could be observed obviously in the XRD pattern of the graphene nanosheets, while it could not be seen in the XRD pattern of the graphene oxide. On the other hand, in the XRD pattern of the graphene oxide, there is another diffraction peak at about 9.8°, which is the characteristic peak of graphene oxide and consistent with those reported in the literatures [43]. These results demonstrate that graphene nanosheets are successfully prepared through the chemical reduction of graphene oxide.

Figure 2 shows the images about the dispersion (1 mg mL^{-1}) of graphene nanosheets and PMo_{12}-functionalized graphene nanosheets (PMo_{12}-Graphene) in aqueous solution, respectively. The suspension of PMo_{12}-Graphene in pure water placed for overnight after ultrasonic treatment was still a homogeneous black dispersion (Fig. 2b). In comparison, the dispersion of graphene nanosheets without PMo_{12} modification produced black precipitation at the bottom of the bottle (Fig. 2a). This demonstrates that PMo_{12} improves obviously the dispersion of graphene nanosheets in water, which is helpful for PtRu nanoparticles to adhere to the graphene nanosheets.

Figure 3 shows TEM images of the PtRu/Graphene (Fig. 3a) and PtRu/PMo_{12}-Graphene catalysts (Fig. 3b). From Fig. 3a and b, it is confirmed that the graphene nanosheets are decorated successfully with dense PtRu nanoparticles. Noteworthy is that no nanoparticle aggrega-

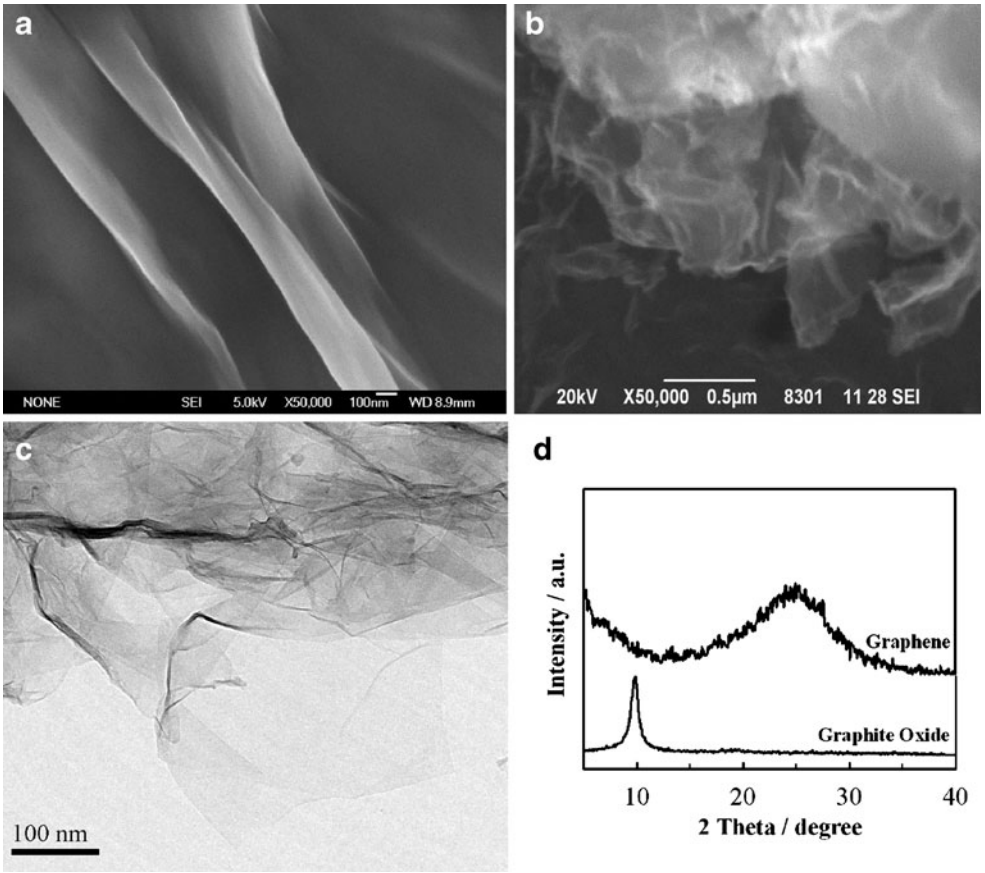

Fig. 1 SEM images of graphene oxide (**a**) and graphene nanosheets (**b**); TEM image of graphene nanosheets (**c**) and XRD patterns of graphene nanosheets and graphene oxide (**d**)

tion is observed on the PMo_{12}-functionalized graphene nanosheets and PtRu nanoparticles with a mean diameter of ca. 2.0 nm disperse uniformly on the graphene nanosheet surface (Fig. 3b). However, for the graphene nanosheets without PMo_{12} modification, the aggregation and larger particle size of PtRu nanoparticles with a mean diameter of ca. 2.5 nm on the surface of graphene nanosheets can be observed (Fig. 3a). This should be attributed to the existence of electrostatic repulsive and coordination interactions between the negatively charged PMo_{12} film on the surface of the graphene nanosheets and the metal particles. EDS analysis was conducted to verify the presence of PMo_{12} in the PMo_{12}-Graphene (Fig. 3c).

Fig. 2 Images about the dispersion (1 mg mL^{-1}) of graphene nanosheets (**a**) and PMo_{12}-functionalized graphene nanosheets (**b**) in aqueous solution

Electrocatalytic activity for methanol oxidation

The catalytic properties of the as-prepared catalysts towards the methanol oxidation reaction were evaluated in 0.5 M H_2SO_4+1.0 M CH_3OH aqueous solution by cyclic voltammetry (CV) at a scan rate of 50 mV s^{-1}, and the corresponding results are shown in Fig. 4. From Fig. 4a, two oxidation peaks, which are related to the oxidation of methanol and the corresponding intermediates produced during the methanol oxidation, can be observed obviously at 0.65 and 0.43 V, respectively. The characteristics of CV curves are in agreement with other works [44]. It is noted that, comparing with the PtRu/Graphene catalyst, the significant enhancement of the peak current of methanol oxidation can be observed on the PtRu/PMo_{12}-Graphene catalyst. The forward peak current density of methanol oxidation on the PtRu/PMo_{12}-Graphene catalyst is

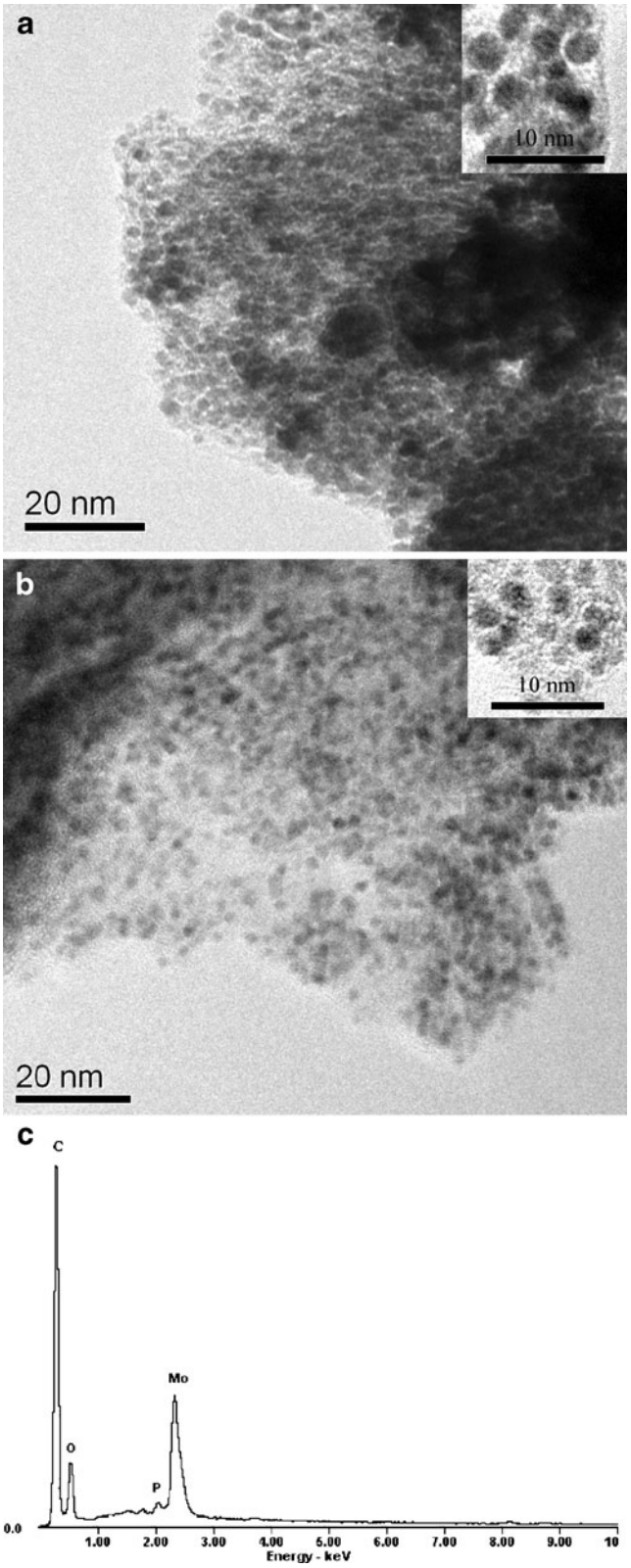

Fig. 3 TEM images of PtRu/Graphene catalysts (**a**) and PtRu/PMo_{12}-Graphene catalysts (**b**); EDS pattern of the PMo_{12}-functionalized graphene nanosheets (**c**)

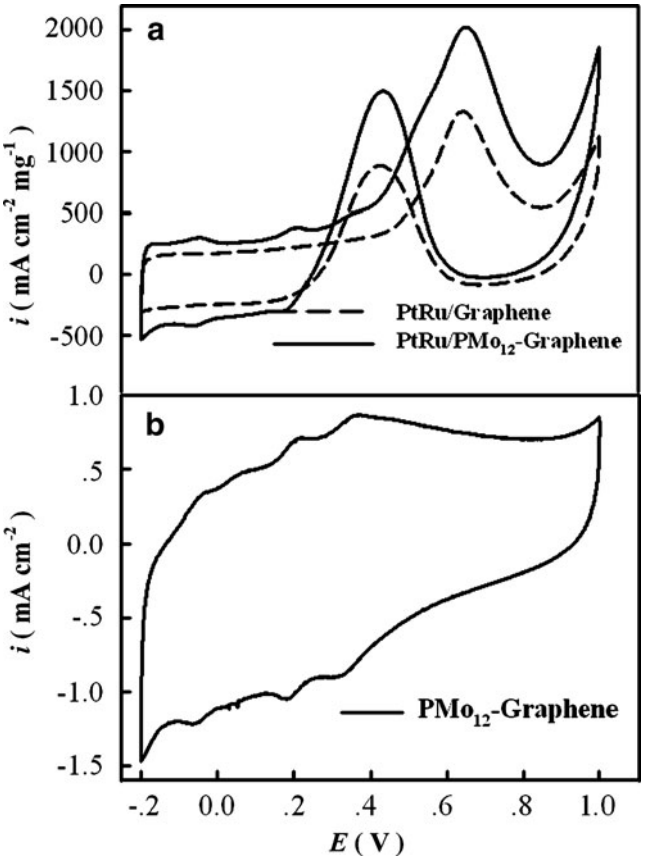

Fig. 4 Cyclic voltammograms of the PtRu/PMo_{12}-Graphene/GC and PtRu/Graphene/GC electrode (**a**) and the PMo_{12}-Graphene/GC electrode (**b**) at 50 mV s^{-1} in 0.5 M H_2SO_4+1.0 M CH_3OH aqueous solution

2,028 mA cm^{-2} mg^{-1}, being 1.5 times higher than that on the PtRu/Graphene catalyst (1,346 mA cm^{-2} mg^{-1}), and better than the results reported in the literature [17]. These show that the electrocatalytic activity of the PtRu/PMo_{12}-Graphene catalyst for methanol oxidation, in terms of mass specific current densities, is better than that of the PtRu/Graphene catalyst and the electrocatalytic activity of the PtRu/Graphene catalyst is enhanced obviously by PMo_{12} modification of graphene nanosheets. In addition, the background current of the PtRu/PMo_{12}-Graphene catalyst at intermediate potential associated with the double layer capacitance of the electrode is much higher than that of PtRu/Graphene, due to the presence of PMo_{12} [45, 46].

To clarify the mechanism about how PMo_{12} improves the electrocatalytic activity of the PtRu/Graphene catalyst, cyclic voltammogram of PMo_{12}-Graphene catalyst for methanol oxidation in 0.5 M H_2SO_4+1.0 M CH_3OH aqueous solution is also shown in Fig. 4b. As seen in Fig. 4b, there is no obvious methanol oxidation peak for Graphen-PMo_{12}. However, three pair of peaks of PMo_{12}, similar with the peaks of the PtRu/PMo_{12}-Graphene catalysts at the same potential window during methanol

oxidation, can be clearly observed at about 0.0, 0.2, and 0.35 V, respectively. These peaks could be attributed to consecutive, approximately two electron redox reactions [47]. The result indicates that the pure PMo_{12} adsorbed stably on graphene nanosheets has no catalytic activity for methanol oxidation, but contributes to the methanol oxidation combining with PtRu nanoparticles. This can be further confirmed from the results of chronoamperometry (CA) shown in Fig. 5. It is observed that during the whole time, the current density of methanol oxidation at the PtRu/PMo_{12}-Graphene/GC electrode is higher than that at the PtRu/Graphene/GC electrode, which is consistent with the results from CV (Fig. 4a).

To further investigate the role of PMo_{12}, the specific electrochemically active surface areas (EAS) of PtRu/PMo_{12}-Graphene and PtRu/Graphene were estimated from the charge associated to the CO_{ads} stripping peak (determined in 0.5 mol L^{-1} H_2SO_4 solution at a scan rate of 50 mV s^{-1} and corrected for the effects of double layer charging currents and oxide growth), and assuming that one monolayer of adsorbed CO linearly bonded requires 0.42 mC cm^{-2} for its oxidation [48]. Figure 6 corresponds to the CO-stripping curves (initiated in the anodic direction) during the first two cycles after the PtRu/PMo_{12}-Graphene (Fig. 6a) and PtRu/Graphene (Fig. 6b) catalysts were pre-absorbed with CO for 20 min. As the scanning progressed, anodic peaks (real line) corresponding to the oxidation of CO_{ads} could be observed from Fig. 6. In the following cycle, the curves are almost overlapped with the stable cycles before pre-adsorption (dashed lines), which indicates that the pre-adsorbed CO on the catalyst surface was completely unabsorbed during the first cycle. From Fig. 6, the calculated EAS values for PtRu/PMo_{12}-Graphene and

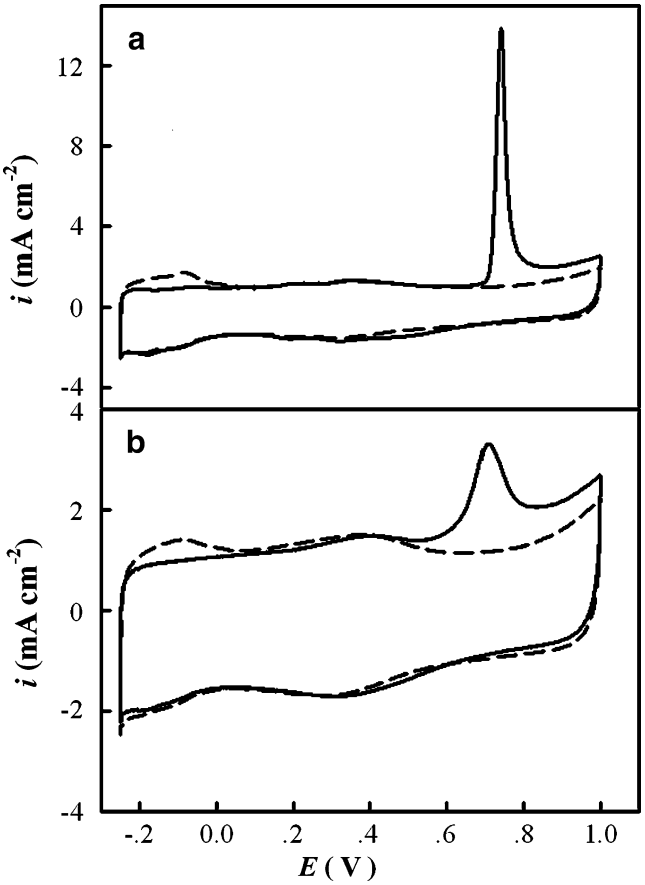

Fig. 6 Cyclic voltammograms of the PtRu/PMo_{12}-Graphene/GC (**a**) and PtRu/Graphene/GC (**b**) electrodes at 50 mV s^{-1} in 0.5 M H_2SO_4 aqueous solution. *Dashed lines* represent the stable cycles before CO pre-adsorption and the *solid lines* represent the first cycle of pre-adsorbed CO oxidation

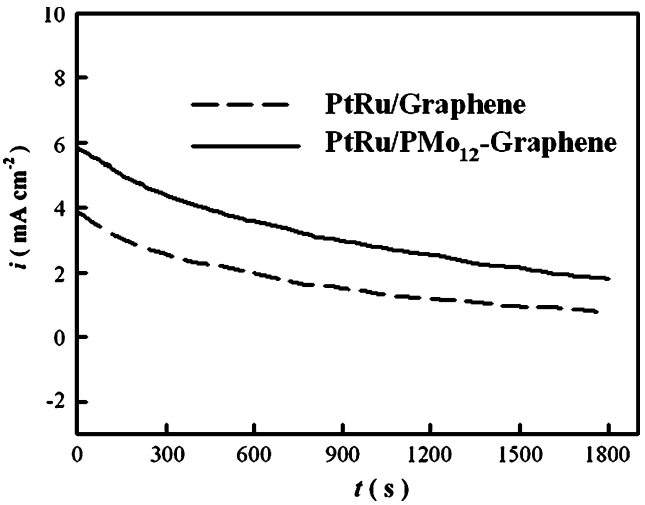

Fig. 5 Chronoamperograms of the PtRu/PMo_{12}-Graphene/GC and PtRu/Graphene/GC electrodes at 0.5 V in 0.5 M H_2SO_4+1.0 M CH_3OH aqueous solution

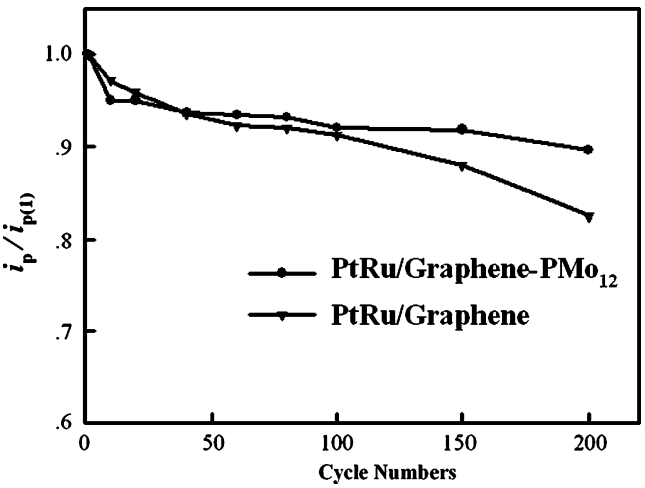

Fig. 7 Long-term cycle stabilities of the PtRu/PMo_{12}-Graphene/GC and PtRu/Graphene/GC electrodes in 0.5 M H_2SO_4+1.0 M CH_3OH aqueous solution at 50 mV s^{-1}

for PtRu/Graphene are 48.05 and 15.90 m^2 g^{-1} of Pt, respectively. It is obvious that the EAS value of the PtRu/PMo_{12}-Graphene catalyst is much higher than that of the PtRu/Graphene.

From a more basic chemical point of view, the specific surface activities of the catalysts, in terms of specific current density normalized to the EAS, were also evaluated, and the calculated specific surface activities for PtRu/PMo_{12}-Graphene and for PtRu/Graphene are 13.0 and 21.7 A m^{-2}, respectively. It is noted that the specific surface activity of PtRu/PMo_{12}-Graphene is slightly lower than that of PtRu/Graphene. The reason is not yet clear, however, the specific current activity of PtRu/Graphene in terms of mass specific currents is improved by PMo_{12}, which is important from a practical point of view.

Based on the results from TEM images (Fig. 3), cyclic voltammograms (Fig. 4) and the above EAS values, the main reasons for the high electrocatalytic activity of the PtRu/PMo_{12}-Graphene catalyst in terms of mass specific currents may be the small particle size, uniform distribution, and high electrochemically active surface area of the PtRu catalyst supported on the PMo_{12}-functionalized graphene nanosheets. Besides, PMo_{12} adsorbed on graphene nanosheets may interact with absorbed hydrogen atoms to form mixed hydrogen/Mo adsorption layers [38], and provide an ideal interface structure on the redox sites with high protonic conductivity [49], thus improving the properties of the PtRu electrocatalyst.

Long-term cycling stability

The long-term cycling stabilities of the PtRu/PMo_{12}-Graphene and PtRu/Graphene catalysts were also investigated in 0.5 M H_2SO_4+1.0 M CH_3OH aqueous solution by cycle voltammetry and the corresponding results are shown in Fig. 7. From Fig. 7, the value of $i_p/i_{p(1)}$ (the ratio between the current densities of the forward oxidation peak at the corresponding cycles and the first cycle) decreases gradually with the continuous scans. This may be due to the accumulation of the intermediates on the catalyst surface, which results in poisoning of the Pt surface and diminution of its activity for methanol oxidation. Also, maybe a change of the surface structure of the PtRu nanoparticles [50] and methanol consumption during the successive scans explains the loss of the current density. When the potential was cycled continuously for 200 cycles, 10.1% loss of the current density at the PtRu/PMo_{12}-Graphene/GC electrode can be observed. However, for the PtRu/Graphene/GC electrode, a larger decrease (18.0%) is observed. The results above imply that the PtRu/PMo_{12}-Graphene catalyst has better long-term cycle stability for methanol oxidation than the PtRu/Graphene catalyst, and the existence of PMo_{12} can enhance the long-term cycle stability of the catalyst.

Conclusions

Well-dispersed PtRu metal nanoparticles were successfully loaded on the PMo_{12}-functionalized graphene nanosheets with microwave heating. The results from TEM, cyclic voltammetries, and the electrochemical surface area indicated that PMo_{12}-Graphene is a good support for PtRu, and the resulting PtRu/PMo_{12}-Graphene catalyst has higher activity, and better cycle stability for methanol electrooxidation comparing with that of the PtRu/Graphene catalyst.

Acknowledgment This work was financially supported by NSFC (20975033), the Program for Fu-Rong Scholar in Hunan Province, China and the Fundamental Research Funds for the Central Universities, China (531107040002).

References

1. Liu H, Song C, Zhang L, Zhang J, Wang H, Wilkinson DP (2006) A review of anode catalysis in the direct methanol fuel cell. J Power Sources 155:95–110
2. Stoupin S, Chung EH, Chattopadhyay S, Segre CU, Smotkin ES (2006) Pt and Ru X-ray absorption spectroscopy of PtRu anode catalysts in operating direct methanol fuel cells. J Phys Chem B 110:9932–9938
3. Rohson DR, Hagans PL, Swider KE, Long JW (1999) Role of hydrous ruthenium oxide in Pt–Ru direct methanol fuel cell anode electrocatalysts: the importance of mixed electron/proton conductivity. Langmuir 15:774–779
4. Chan KY, Ding J, Ren JW, Cheng SA, Tsang KY (2004) Supported mixed metal nanoparticles as electrocatalysts in low temperature fuel cells. J Mater Chem 14:505–516
5. Spinace E, Neto AO, Linardi M (2004) Electro-oxidation of methanol and ethanol using PtRu/C electrocatalysts prepared by spontaneous deposition of platinum on carbon-supported ruthenium nanoparticles. J Power Sources 129:121–126
6. Tsai Y-C, Hong Y-H (2008) Electro-chemical deposition of platinum nanoparticles in multiwalled carbon nanotube—Nafion composite for methanol electro-oxidation. J Solid State Electrochem 12:1293–1299
7. Matsumoto T, Komatsu T, Arai K, Yamazaki T, Kijima M, Shimizu H, Takasawa Y, Nakamura J (2004) Reduction of Pt usage in fuel cell electrocatalysts with carbon nanotube electrodes. Chem Commun 7:840–841
8. Steigerwalt ES, Deluga GA, Lukehart CM (2002) Pt–Ru/carbon fiber nanocomposites: synthesis, characterization, and performance as anode catalysts of direct methanol fuel cells. A search for exceptional performance. J Phys Chem B 106:760–766
9. Chai GS, Yoon SB, Yu JS (2005) Highly efficient anode electrode materials for direct methanol fuel cell prepared with ordered and disordered arrays of carbon nanofibers. Carbon 43:3028–3031
10. Yoshitake T, Shimakawa Y, Kuroshima S, Kimura H, Ichihashi T, Kubo Y (2002) Preparation of fine platinum catalyst supported on single-wall carbon nanohorns for fuel cell application. Physica B 323:124–126
11. Su F, Zhao XS, Wang Y, Zeng J, Zhou Z, Lee JY (2005) Synthesis of graphitic ordered macroporous carbon with a three-dimensional interconnected pore structure for electrochemical applications. J Phys Chem B 109:20200–20206

12. Yu JS, Kang S, Yoon SB, Chai G (2002) Fabrication of ordered uniform porous carbon networks and their application to a catalyst supporter. J Am Chem Soc 124:9382–9383
13. Liu Y, Qiu X, Huang Y, Zhu W, Wu G (2002) Influence of preparation process of MEA with mesocarbon microbeads supported Pt–Ru catalysts on methanol electrooxidation. J Appl Electrochem 32:1279–1285
14. Joo SH, Lee HI, You DJ, Kwon K, Kim JH, Choi YS, Kang M, Kim JM, Pak C, Chang H, Seunga D (2008) Ordered mesoporous carbons with controlled particle sizes as catalyst supports for direct methanol fuel cell cathodes. Carbon 46:2034–2045
15. Geim AK, MacDonald AH (2007) Graphene: exploring carbon flatland. Phys Today 60:35–41
16. Peigney A, Laurent C, Flahaut E, Bacsa RR, Rousset A (2001) Specific surface area of carbon nanotubes and bundles of carbon nanotubes. Carbon 39:507–514
17. Dong LF, Gari R, Li Z, Craig MM, Hou SF (2010) Graphene-supported platinum and platinum–ruthenium nanoparticles with high electrocatalytic activity for methanol and ethanol oxidation. Carbon 48:781–787
18. Xu C, Wang X, Zhu JW (2008) Graphene–metal particle nanocomposites. J Phys Chem, C 112:19841–19845
19. Li YM, Tang LH, Li JH (2009) Preparation and electrochemical performance for methanol oxidation of pt/graphene nanocomposites. Electrochem Commun 11:846–849
20. Yoo EJ, Okata T, Akita T, Kohyama M, Nakamura J, Honma I (2009) Enhanced electrocatalytic activity of Pt subnanoclusters on Graphene nanosheet surface. Nano Lett 9:2255–2259
21. Bian J, Xiao M, Wang SJ, Lu YX, Meng YZ (2009) Graphite oxide as a novel host material of catalytically active Cu–Ni bimetallic nanoparticles. Catal Commun 10:1529–1533
22. Wang X, Zhi LJ, Müllen K (2008) Transparent, conductive graphene electrodes for dye-sensitized solar cells. Nano Lett 8:323–327
23. Hummers WS, Offeman JRE (1958) Preparation of graphitic oxide. J Am Chem Soc 80:1339
24. Saito Y, Kitamura T, Wada Y, Yanagida S (2002) Poly(3, 4-ethylenedioxy- thiophene) as a hole conductor in solid state dye sensitized solar cells. Synth Met 131:185–187
25. Mende LS, Grätzel M (2006) TiO2 pore-filling and its effect on the efficiency of solid-state dye-sensitized solar cells. Thin Solid Films 500:296–301
26. Niyogi S, Bekyarova E, Itkis ME, McWilliams JL, Hamon MA, Haddon RC (2006) Solution properties of graphite and graphene. J Am Chem Soc 128:7720–7721
27. Wang G, Yang J, Park J, Gou X, Wang B, Liu H, Yao J (2008) Facile synthesis and characterization of graphene nanosheets. J Phys Chem, C 112:8192–8195
28. Si YC, Samulski ET (2008) Synthesis of water soluble graphene. Nano Lett 8:1679–1682
29. Xu YX, Bai H, Lu GW, Li C, Shi GQ (2008) Flexible graphene films via the filtration of water-soluble noncovalent functionalized graphene sheets. J Am Chem Soc 130:5856–5857
30. Stankovich S, Dikin DA, Dommett GH, Kohlhaas KM, Zimney EJ, Stach EA, Piner RD, Nguyen ST, Ruoff RS (2006) Graphene-based composite materials. Nature 442:282–286
31. Liu H, Gao J, Xue MQ, Zhu N, Zhang MN, Cao TB (2009) Processing of graphene for electrochemical application: non-covalently functionalize graphene sheets with water-soluble electroactive methylene green. Langmuir 25:12006–12010
32. Ferrell JR, Kuo MC, Turner JA, Herring AM (2008) The use of the heteropoly acids, $H_3PMo_{12}O_{40}$ and $H_3PW_{12}O_{40}$, for the enhanced electrochemical oxidation of methanol for direct methanol fuel cells. Electrochim Acta 53:4927–4933
33. Maiyalagan T (2009) Silicotungstic acid stabilized Pt–Ru nanoparticles supported on carbon nanofibers electrodes for methanol oxidation. Int J Hydrogen 34:2874–2879
34. Seo MH, Choi SM, Kim HJ, Kim JH, Cho BK, Kim WB (2008) A polyoxometalate-deposited Pt/CNT electrocatalyst via chemical synthesis for methanol electrooxidation. J Power Sources 179:81–86
35. Kuhn A, Anson FC (1996) Adsorption of monolayers of $P_2Mo_{18}O_{62}^{6-}$ and deposition of multiple laKyers of $Os(bpy)_3^{2+}$–$P_2Mo_{18}O_{62}^{6-}$ on electrode surfaces. Langmuir 12:5481–5488
36. Ge M, Zhong B, Klemperer WG, Gewirth AA (1996) Self-assembly of silicotungstate anions on silver surfaces. J Am Chem Soc 118:5812–5913
37. Pan DW, Chen JH, Tao WY, Nie LH, Yao SZ (2006) Polyoxometalate-modified carbon nanotubes: new catalyst support for methanol electro-oxidation. Langmuir 22:5872–5876
38. Han DM, Guo ZP, Zeng R, Kim CJ, Meng YZ, Liu HK (2009) Multiwalled carbon nanotube-supported Pt/Sn and Pt/Sn/PMo_{12} electrocatalysts for methanol electro-oxidation. J Hydrogen Energy 34:2426–2434
39. Gilje S, Han S, Wang MS, Wang KL, Kaner RB (2007) A chemical route to graphene for device applications. Nano Lett 7:3394–3398
40. Stoller MD, Park S, Zhu YW, An J, Ruoff RS (2008) Graphene-based ultracapacitors. Nano Lett 8:3498–3502
41. Wang GX, Wang B, Park J, Yang J, Shen XP, Yao J (2009) Synthesis of enhanced hydrophilic and hydrophobic graphene oxide nanosheets by a solvothermal method. Carbon 47:68–72
42. Stankovich S, Piner RD, Chen XQ, Wu NQ, Nguyen ST, Ruoff RS (2006) Stable aqueous dispersions of graphitic nanoplatelets via the reduction of exfoliated graphite oxide in the presence of poly(sodium 4-styrenesulfonate). J Mater Chem 16:155–158
43. Nethravathi C, Rajamathi M (2008) Chemically modified graphene sheets produced by the solvothermal reduction of colloidal dispersions of graphite oxide. Carbon 46:1994–1998
44. Prader DN, Rusek JJ (2003) Energy density of a methanol/hydrogen-peroxide fuel cell. Appl Energy 74:135–140
45. Guo ZP, Han DM, Wexler D, Zeng R, Yao SZ (2008) Polyoxometallate-stabilized platinum catalysts on multi-walled carbon nanotubes for fuel cell applications. Electrochim Acta 53:6410–6416
46. Han DM, Guo ZP, Zhao ZW, Zeng R, Meng YZ, Shu D (2008) Polyoxometallate-stabilized Pt–Ru catalysts on multiwalled carbon nanotubes: influence of preparation conditions on the performance of direct methanol fuel cells. J Power Sources 184:361–369
47. Kulesza PJ, Chojak M, Karnicka K, Miecznikowski K, Palys B, Lewera A, Wieckowski A (2004) Network films composed of conducting polymer-linked and polyoxometalate-stabilized platinum nanoparticles. Chem Mater 16:4128–4134
48. Alcaide F, Miguel Ó, Grande H-J (2006) New approach to prepare Pt-based hydrogen diffusion anodes tolerant to CO for polymer electrolyte membrane fuel cells. Catal Today 116:408–414
49. Minoru O, Tsuyohiko F, Naotoshi N (2009) Design of an assembly of Poly(benzimidazole), carbon nanotubes, and Pt nanoparticles for a fuel-cell electrocatalyst with an ideal interfacial nanostructure. Small 5:735–740
50. Haruta M, Date M (2001) Advances in the catalysis of Au nanoparticles. Appl Catal, A 222:427–437